Salzburg University
of Applied Sciences

Oregon State University
College of Forestry

Mass Plywood Panels

Performance, Design and Application

AUTHOR

BENJAMIN STRASSER

1710556063

Presented in the Month of September

Supervisor Home University

FH-Prof. Univ.-Prof. Dr.-Ing. Dr. Marius-Catalin Barbu

Supervisor Host University

Lech Muszynki Ph.D

Bachelor's programme: Forest Products Technology and Wood Constructions

Technology

Health

Media

Acknowledgements

Abstract

To determine the increase of the added value of trees with small cross section, it should be examined whether these are suitable for the use as core lamellas in the production of cross-laminated timber boards. For this purpose, boards will be produced whose core lamellas gradually decrease in width. These boards will then be cut up into samples, which will be subjected to a non-destructive bending test as well as to a failure test. A Linear Variable Differential Transformer is used to eliminate the compressions and the resulting more accurate results during the non-destructive test series. The results of these tests are then compared with the values of the PRG 320 to determine whether the corresponding minimum requirements are met. After evaluation of the data and comparison of the PRG values, it showed that very good results were achieved, especially for the bending stiffness, which for the most part exceed the limit values. For the modulus of elasticity, on the other hand, the results cover a wide range, which is why a new test series would be recommended.

Cross Laminated Timber, bending test, Modulus of Elasticity, Modulus of Rupture, Linear Variable Differential Transformer (LVDT)

Für die Erhöhung der Wertschöpfung von Bäumen mit geringem Querschnitt soll überprüft werden, ob diese für die Verwendung als Kern Lamellen bei der Produktion von Brettsperrholz Platten in Frage kommen. Dafür werden Platten hergestellt werden, deren Kern Lamellen in der Breite sukzessive abnehmen. Diese Platten werden anschließend auf Proben aufgetrennt, welche sowohl einer zerstörungsfreien Biegeprüfung unterzogen werden als auch einer bis zum Versagen. Zur Ausklammerung der Kompressionen und der daraus akkurateren Ergebnisse im Zuge der zerstörungsfreien Testserie, wird ein Linear Variable Differential Transformer eingesetzt. Die Ergebnisse dieser Prüfungen sind im weiteren Verlauf mit den Werten der PRG 320 zu vergleichen, um zu erheben, ob die entsprechenden Mindestanforderungen erfüllt werden. Nach Auswertung der Werte und der Gegenüberstellung der Vergleichswerte, zeigt sich, dass speziell bei der Biegesteifigkeit sehr gute Ergebnisse erzielt werden, welche die Grenzwerte zum größten Teil übersteigen. Beim Elastizitätsmodul hingegen umfassen die Ergebnisse eine breite Streuung, weshalb eine erneute Testserie zu empfehlen wäre.

Brettsperrholz, Biegeprüfung, Elastizitätsmodul, Biegesteifigkeit, Differentialtransformator

Index

1   Intro

Whether caused by natural events such as lightning or human influence, forest fires can cause considerable damage both economically and ecologically. In order to prevent this, appropriate measures are taken. This includes the preventive clearing of forests or parts of forests. Should a fire actually occur, there's good potential to spread and burn wide swahs of land. However, this results in a lot of round timber, which is not attractive according to the current state of the timber industry, as the trees are often still too young and therefore do not reach a sufficient diameter. This leads to the fact that often they are only supplied to the panel or pulp industry and therefore are very close to the end of the value chain. For a more sustainable use of this valuable raw material, it is essential to use it in such a way that it can be used over a long period of time and several stages in the recycling economy are still utilized. The engineer wood material "Cross laminated timber - CLT" could be suitable for this purpose.

1.1   Motivation

Due to its extensive fields of application, this building product has enjoyed a considerable increase in the construction industry in recent years. The corresponding production facilities are concentrated in the Alpine region in Europe, where Austria is considered the main player. Looking at CLT's market development, it is clear that there is no foreseeable break in the growing demand over the next few years. Therefore, the current market leaders are trying to open up new markets on the one hand and to jump on this bandwagon more and more on the other hand. This, however, also means that wood as a material is becoming more strongly and fiercely contested as well. Therefore, an optimization for the corresponding engineered wood-based panels is desirable from both an ecological and economic point of view. For this purpose, those trees could be used which are not attractive for the production of such engineered wood according to the current state of the art.

1.2   Background

Cross-laminated timber (CLT) was developed in the early 1990s and Central Europe is recognized as the birthplace. CLT is an Engineered Wood Product (EWP), which usually consists of 3 to 9 layers of boards, each layer being arranged at 90 degrees to each other. These layers are connected with each other in a friction-locked manner, creating a load-bearing element. The bonding of the individual layers with suitable adhesives is most common. They can also be joined with nails made of wood, aluminum, or other materials. The

field of application includes all kinds of building components such as walls, ceilings, and roof elements.

Boards with a thickness of 16 to 51mm are used for the production of CLT panels. Furthermore, the thickness of the individual layers should not differ among themselves. The width of the lamellas of the top layers should be at least 1.75 times the lamella thickness. For the core lamellas, the ratio of lamella width to lamella thickness should not be less than 3.5 (PRG 320:2019).

1.3 Hypothesis

For the ecological and sustainable use of small diameter logs, which are increasingly being used for preventive logging to contain forest fires, CLT panels could have great potential. This applies in particular to the middle layer of such panels. From a static point of view, the core lamellas have a very minor effect on the bending stress. The reason for this is that the core lamellas represent the zero line and therefore no or only very low tensile and compressive stresses occur at the edges of these lamellas. If one looks at the basic values of the PRG 320 for the bending strength of 3-layer structures, for example, this is clearly evident. For example, the ratio between the values for the main load-bearing direction and the secondary load-bearing direction is 28:1 to 37:1 for the USA and 26:1 to 34:1 for Canada.

The shear stiffness, on the other hand, is somewhat lower in the main load-bearing direction than in the secondary load-bearing direction. According to PRG 320, a ratio of 1:1.06 to 1:1.08 for the American market and 1:1.03 to 1:1.24 for Canada is given as the base value (PRG 320:2019).

1.4 Objectives

In order to examine this consideration in more detail, samples with core lamellas of different widths are to be produced and then subjected to both non-destructive and destructive 3-point bending tests. The test results will then be evaluated and compared to the standard PRG 320 to determine whether narrower core lamellas can be used in the production of CLT panels.

2   Materials & Methods

The production of the plates, the separation into the individual samples, as well as the first run of the non-destructive 3-point bending tests and the corresponding data evaluation were carried out in summer 2018 (Prox Lauren et al. 2018).

2.1   Raw material (species, dimensions, …)

CLT panels are manufactured for testing in the company's own workshops. The reason for this is that the core lamellas within a panel vary in width and such panels are not available as prefabricated panels.

2.1.1   Wood

Southern Yellow Pine is used for the plates. However, this is not a specific wood species, but a group usually consisting of Loblolly Pine (Pinus taeda), Long Leaf Pine (Pinus palustris), Short Leaf Pine (Pinus echinata) and Slash Pine (Pinus eliotti). The average MOE is given as 8,900 MPa. The MOR has a size of 65.000 kPa The specific gravity is 0,40 according to literature, these values refer to a moisture content of 12% (Ross; USDA Forest Service. 2010).

2.1.2   Resin

A 2-component resin is used to connect the individual lamella layers over the entire surface. This consists of the phenol formaldehyde resorcinol resin „*Cascophen® LT-75C*" and the catalyst „*Cascoset® FM-282*". Please refer to the manufacturer's Safety Data Sheets (annex 2+3)

2.2   Fabrication

Compliance with safety regulations is a top priority for the production of the boards. For this, please refer to the SOP for CLT production of the Department of Wood Science & Engineering (annex 1).

2.2.1   Plane

Before starting production, the wood must be calibrated to ensure a flat and even surface for the resin application and the subsequent pressing process. In order to obtain a finished depth of the panels and the samples to be obtained, averaging 70.5 mm, the boards are calibrated to an average thickness of 23.5 mm.

Figure 1: planing of lamellas
Source: (SOP for CLT fabrication, 2018)

2.2.2 Preparation of core Lamellas

Since the influence of the width of the core lamellas on the mechanical properties is to be investigated, the core lamellas are divided into three widths. In order to minimize distortion caused by different boards and the associated deviations in fiber direction, number of growth rings, and growth ring width, the core lamellas are cut to the corresponding widths. This means that boards are prepared with a length that corresponds to the width of an entire panel. Then the length is theoretically divided into three. Finally, a band saw is used to cut them once up to the imaginary division between the first and second thirds and twice more up to the boundary between the second and third thirds (see figure 2). As a result, the boards of the core lamellas have a width of 140 mm (5.5 in) in the first third, twice 70 mm (2.75 in) in the middle third and four times 35 mm (1.38 in) in the last third, but the wood-specific properties of each board do not vary across the width of the panels.
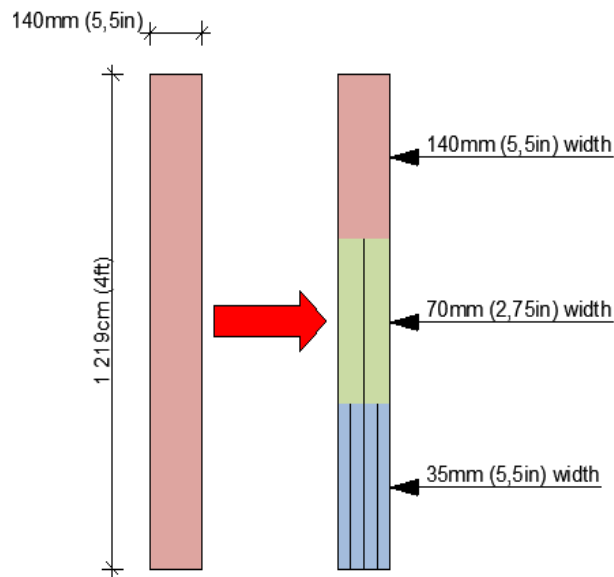
Figure 2: cuts of core lamellas
Source: (separate figure, 2020)

This separation results in the following ratios of width to thickness of the core lamellas.

Table 1: ratio width to depth for core lamella width
source: (own table, 2020)

lamella width	35 mm	70 mm	140 mm
ratio width to depth	1,49	2,98	5,96

This separation results in the following ratios of width to thickness of the core lamellas (PRG 320:2019).

2.2.3 Resin apply and array

As described above, a 2-component adhesive is used. According to the manufacturer, the mixing ratio between resin and catalyst is 100/30. To maintain this ratio, the individual components must be weighed with a laboratory balance with an accuracy of 0.1 g.

The recommended quantity of ready-mixed adhesive is 490 g/m² (100 lb / 1000 ft²). To ensure that this ratio is accurately maintained, each board should be placed individually on a suitable balance, which is then zeroed. Then the appropriate amount of adhesive is applied. Once the desired quantity has been reached, the adhesive is to be distributed evenly.

Figure 3: resin apply and array
Source: (SOP for CLT fabrication, 2018)

After application of the adhesive, the individual boards of the first top layer must be laid out on a suitable and prepared base. Make sure that the glued surface is facing upwards and that it is not touched. As soon as the entire top layer has been laid out, the core lamellas must then be placed on top. Adhesive is not applied to these pieces. When laying the core layers, it is essential to ensure that the separated boards (35mm and 70mm) are laid down in accordance with the corresponding whole boards (140mm) and that these are not interchanged or twisted. Finally, the 2 layers of cover lamellas must be glued in accordance with the 1st layer and distributed over the core lamellas. However, the side with adhesive must be turned in the direction of the core lamellas.

Figure 4: board layup
Source: (SOP for CLT fabrication, 2018)

2.2.4 Pressing

After the application of the adhesive is completed and the lamellas are positioned accordingly, the plate is lifted into the appropriately prepared press with the help of a forklift. Make sure that foil is placed on both the upper and lower side of the plate to prevent the adhesive from contaminating the press. As soon as these precautions have been taken, the press can be closed, making sure that all persons involved keep a sufficient safety distance to prevent injuries from the closing process.

The plates must be pressed with the manufacturer's recommended pressure. The reason for this is twofold, one is to achieve an even setting of the adhesive, and the other is to prevent excessive compression of the boards.

2.2.5 Cut up and labeling

After sufficient time to cool down, the finished pressed plates should be cut to the desired format for the samples to be used later. The finished samples have a dimension of 730mm in length, 154mm in width and 71mm in depth. Afterwards the samples were labeled immediately to prevent confusion. In the first step, 2 plates were divided along the main carrying direction (deck lamellas) into 6 "carriers" each with the finished width of 154mm. This results in a total of 12 "carriers". This numerical designation also describes the first digits of the sample designation (S1 - S12) with an "S" for sample. From these in turn, the samples with the finished length of 762mm (2.5 ft) were then cut. This means that the carriers were divided twice, resulting in 3 samples per carrier. In addition to the numerical designation from 1 to 12, these were extended by an additional alphanumeric digit (A, B and C). Due to an incomprehensible reason, only 2 samples were obtained from one carrier.

In the course of the evaluation of the samples, however, it turned out that the samples have a partially comprehensible labeling along the main carrying direction, but along the secondary carrying direction (core lamellas) the corresponding numbering is ascending, but not, as expected, constant along the secondary carrying direction (e.g.: S11, S12, S2, S4, etc.). Therefore, it was necessary to reconstruct the arrangement of the samples according to the original plates and to create a designation that allows to clearly define the position of the samples in relation to the whole plate.

For the first step, the samples were placed on a sufficiently large surface. Based on the original labeling (e.g. S1A, S1B and S1C), an attempt was made to see if the correct position along the main carrying direction (deck lamellas) corresponds to the sequence of letters from A to C. By examining the grain of the deck lamellas and the annual rings of the associated core lamellas, it was found that the alphanumeric designation does not correspond to a constant sequence. Therefore, as a next step, the samples along the deck lamellas as well as the core lamellas had to be examined and rearranged individually. The arrangement of the original plates could be reconstructed by distinctive features such as annual ring width, knots, or discoloration.

The next task was to develop a labeling system that would allow the samples to be specifically assigned to the position of the respective plate, but also to identify the width of the core layer without additional information. A multi-digit code consisting of a combination of letters and numbers is used for this purpose. For an easier and better traceability the plates were divided into rows and columns, similar to a table software. The "carriers" mentioned at the beginning are considered as rows and the corresponding division of these "carriers" into the individual samples as columns. This results in a total of 6 rows and 3 columns per plate.

The first digit of the code describes which plate it is. Since a total of 3 plates were produced, the letters A, B, and C are used for this purpose. The second digit contains the information of the core plate width. Since the width of the lamellas from 35 to 140 mm takes up too many digits, the number of lamellas in relation to the original boards was used instead. This means that lamellas with a width of 140 mm get the designation 1, those with a width of 70 mm get the designation 2 (2 elements of a whole board) and lamellas with a width of 35 mm get the designation 4 because the corresponding raw lamellas have been divided into 4 parts. This is the first definition of the rows. For the board "A" there are still the "beams", which show the joints of the differently wide core lamellas, i.e. those which lie between the described rows. These are designated with the letters X, Y and Z.

The alphanumeric sequence from A to F is used to define the position of the original "carriers" transverse to the grain direction of the top lamellas.

The columns are classified by means of numbers from 01 to 12, with each sample being defined by 2 numbers. One digit at the left and one at the right end of the samples, starting at the left end of the row and ascending to the right end. This ensures that the samples are not rotated.
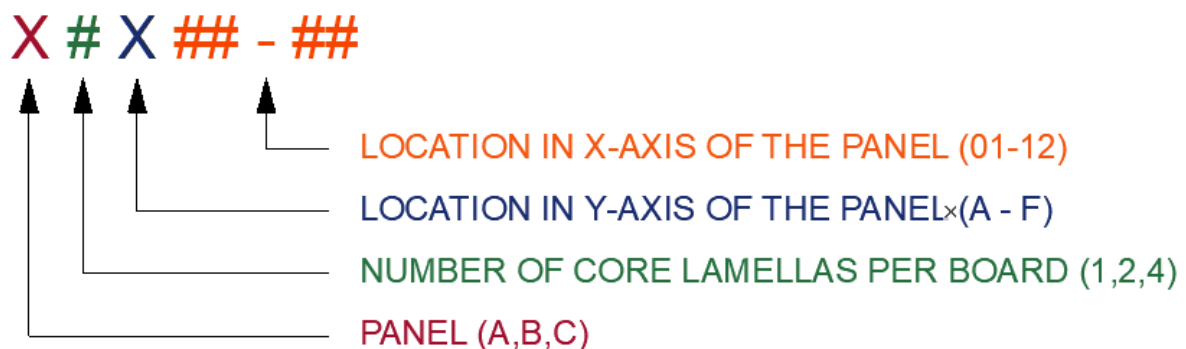

Figure 5: labeling coding for samples
Source: (separate figure, 2020)

It should be noted, however, that for 2 of the 3 panels, those rows with the designations X, Y and Z are no longer available and therefore the grain of the deck lamellas required for classification is not possible. Therefore, it cannot be guaranteed that the sequence of the rows, in relation to the width of the core lamellas, corresponds to the actual position. However, since the core lamellas of the individual samples correspond to those of the adjacent samples, this has no influence on the design of the experiment.

2.3 Storage & conditions

After the first series of experiments was completed in 2018, the samples were stored on a pallet in the laboratory 173. There is no record of room conditioning for this room, so it is not

possible to fully understand what conditions the samples have been exposed to since storage. However, the room is kept at a relatively constant temperature level and relative humidity by the installed ventilation system.

For control purposes, the room conditions in the laboratory where the samples were stored and in the laboratory where the bending tests are performed, are determined over several days with the help of a digital hygrometer. The corresponding values were recorded a maximum of three times per day.
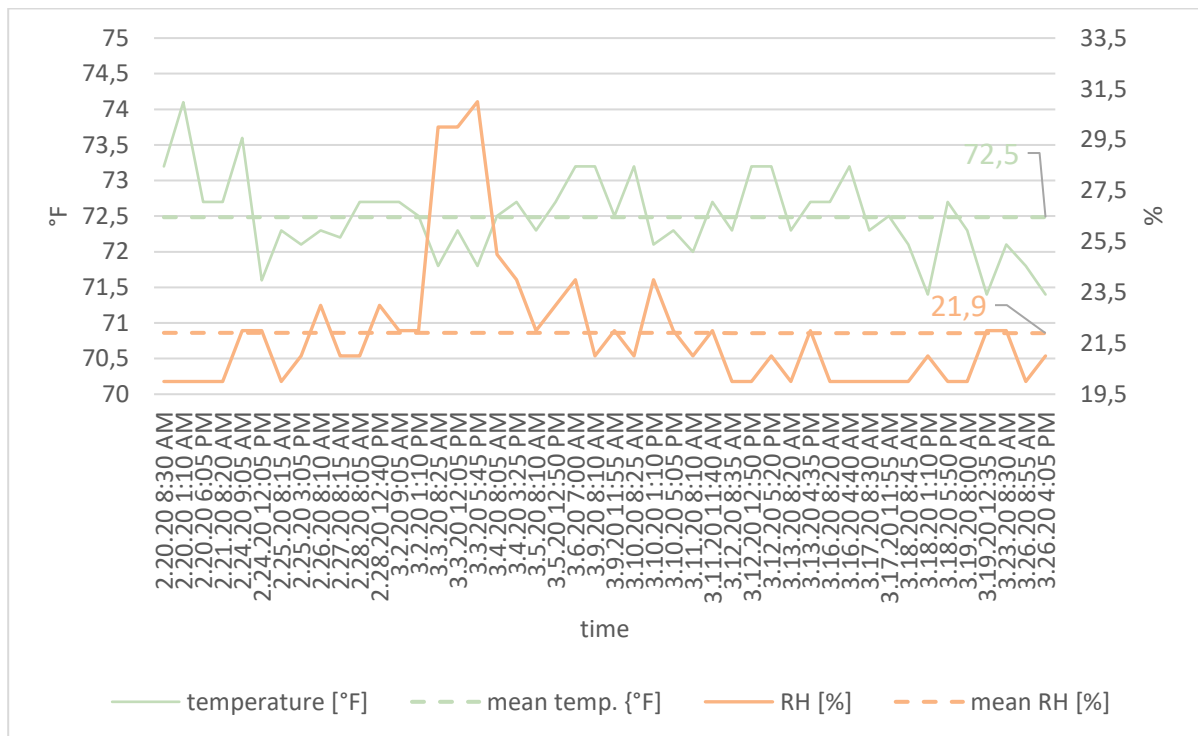

Figure 6: room conditions of pressing laboratory
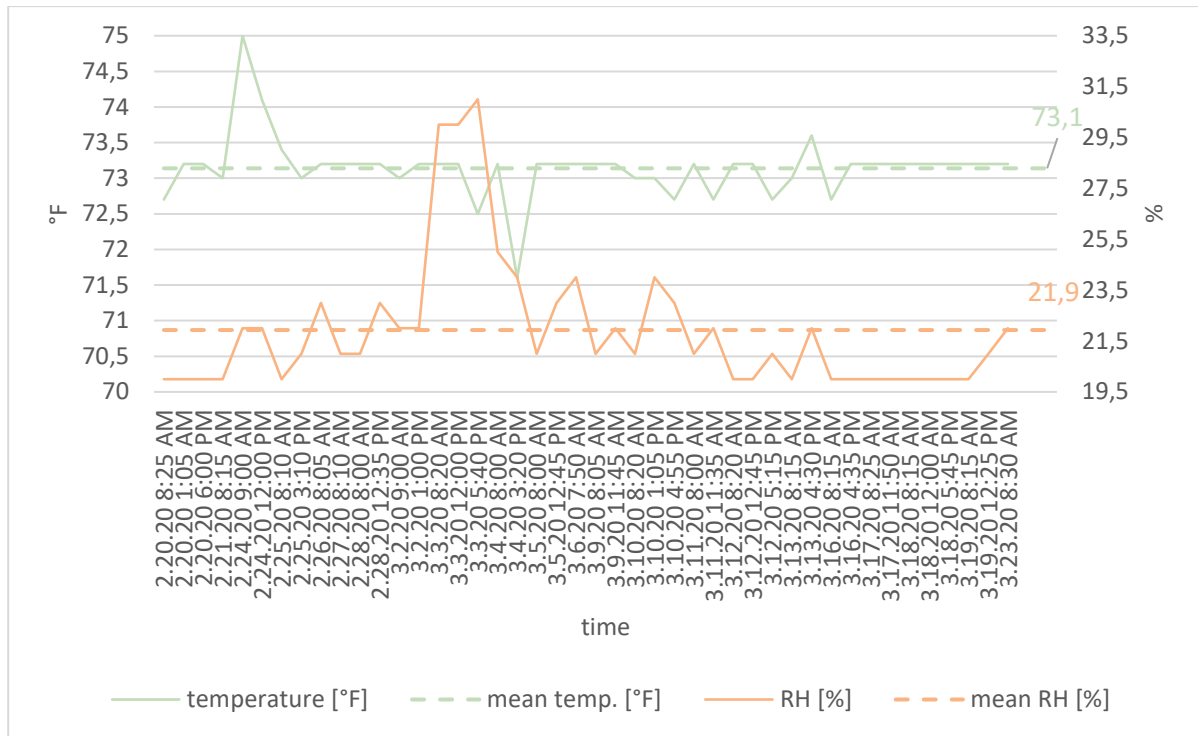*Source: (separate figure, 2020)*

Figure 7: room conditions of storage room
Source: (separate figure, 2020)

Even if there are larger deviations on some days, such as on March 3, 2020, in the long term the average temperature in the testing laboratory will be 72.5°F and the relative humidity 21.9%. In the room (173) in which the samples were stored, the relative humidity has the same value, but the room temperature is on average slightly higher at 73.1°F. Using these values and the formula below, the Equilibrium Moisture Content (EMC) can now be determined.

Formula 1: Calculation of EMC in percent

$$EMC\ (\%) = \frac{1{,}800}{W}\left[\frac{Kh}{1-Kh} + \frac{K_1Kh + 2K_1K_2K^2h^2}{1 + K_1Kh + K_1K_2K^2h^2}\right]$$

T	*temperature in degrees Fahrenheit*
h	*humidity fractional*
W	*330 + 0,452T + 0,00415T^2*
K	*0,791 + 4,63 * 10^{-4}T – 8,44 * $10^{-7}$$T^2$*
K_1	*6,340 + 7,75 * 10^{-4}T – 9,35 * $10^{-5}$$T^2$*
K_2	*1,090 + 2,84 * 10^{-2}T – 9,04 * $10^{-5}$$T^2$*

This results in an EMC of **4.81%** for the samples, with no room difference

2.4   Scale the samples

For further calculations the exact dimensions of the cross sections of the individual samples are important. Therefore, the width and the depth of all samples are determined in addition to the length at both ends. In addition, the depth of the individual lamellas is also determined. Since the boards of the top layers are not butt to butt, this distance is also recorded.

2.5   Setup

The bending tests are performed according to ASTM D198-15.

As already described, the samples have a length of 730mm. During the first series of tests in summer 2018, the samples were tested at a spanlength of 610mm (2 ft), 457mm (1.5 ft) and 305mm (1 ft). In the current test series, the spanlength is 711.2mm (2 ft 4 in).

The following points describe the corresponding equipment, programs, and procedures.

2.5.1   Instron 5582 – Universal Testing System

For the bending tests in summer 2018 as well as for the current ones, a Universal Testing System from Instron is used. This is a "high force" system with the product series 5582.

Figure 8: Universal Testing System – Instron 5582
Source: (separate figure, 2020)

The load cell used is suitable for a maximum load of 100 kN.

Figure 9: 100 kN load cell
Source: (separate figure, 2020)

A steel bar serves as support for the individual samples, on which 2 supports are mounted. Each of these has a bearing roller, which can be moved along the horizontal axis, so that the load bearing block is fully supported, even with asymmetric prisms. The steel bar is freely rotatable in the horizontal plane and is only limited by the load frame.

The force is applied to the carriers with a stamp. Since the pressure bar of the stamp is shorter than the samples are wide, a steel plate is inserted between the stamp and the carrier, which distributes the force over the entire width.

Figure 10: stamp with steel plate
Source: (separate figure, 2020)

2.5.2 Linear Variable Differential Transformer – LVDT

Since the steel plate and bearing roller areas are subject to compression during the bending tests, which can falsify the results of the stress-strain diagram, a Linear Variable Differential Transformer - LVDT is installed. With the help of this and a corresponding aluminum yoke, the adjusted stress-strain diagram can be determined in the zero line. For this purpose, two

screws are screwed into the side surface of the samples along the zero line in the extension of the two supports as supports for the yoke. The yoke is then placed on this surface. Next, a pinboard needle is pressed into the wood in the center of the side surface as an anchor. A string is attached to this anchor, which is connected to the LVDT via a pulley. It is important to ensure that this string is guided vertically downwards from the anchor to avoid distortion of the results. When attaching the LVDT to the aluminum yoke, it must be ensured that the core extension is positioned relatively centrally in the housing and that it can be moved freely and without obstruction. To ensure that the LVDT can also detect the height difference of the anchor point during the bending tests, a second anchor should be provided at the other end of the core extension. This is connected to a fixed point by a rubber band. This keeps the cord and the core extension under constant tension and changes its position only when the samples are bent.
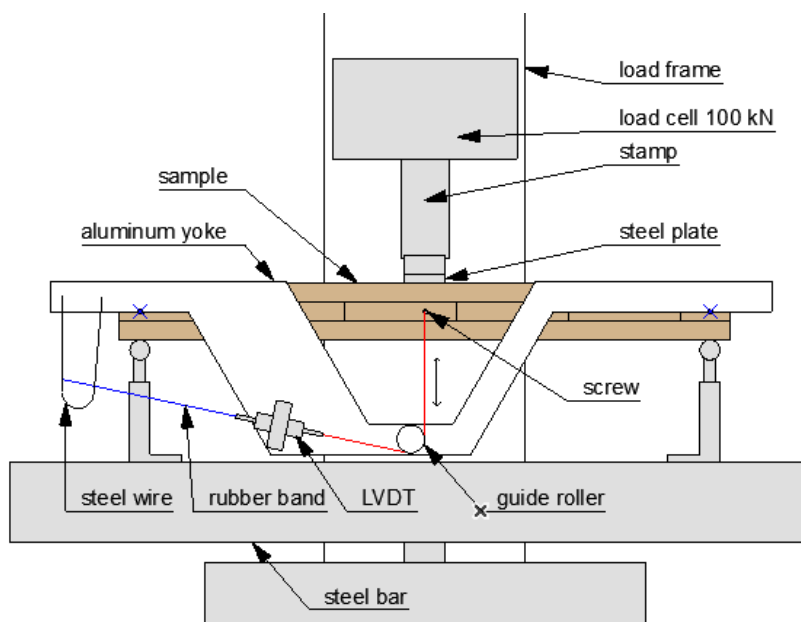

Figure 11: side view of Instron setup combined with LVDT
Source: (separate figure, 2020)

2.5.3 Digital Image Correlation – DIC

With the help of Digital Image Correlation - DIC, the deformation during an experiment can be recorded without contact. This is done by detecting and tracking surface patterns, which are either naturally present or artificially applied. The surface patterns are called sprinkle patterns in the following. The following defined windows are examined (LaVision 2020).
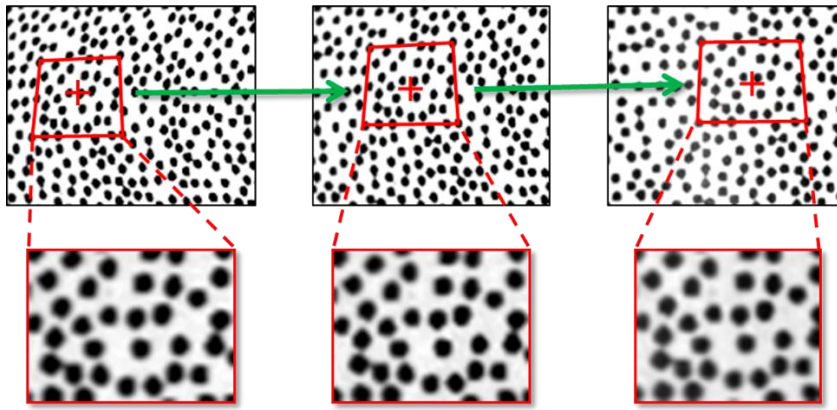
Figure 12: schematic of digital image correlation
Source: (lavision.de, 2020)

In the case of this test series and the associated bending tests, the change in position of individual points of the sprinkle pattern can be recorded. These points should represent the equivalent of the wood fibers of the beams. To detect these changes, the sprinkle pattern is applied to one side of the beam.

During this test series a 3D setup is used. This setup allows the acquisition and calculation of a two-dimensional deformation and subsequently the strain tensors for the examined surface. This process is also called stereoscopic DIC. To make this possible, the use of two cameras is necessary. These simultaneously take images of the surface at different angles. Utilizing the proper calibration for this camera setup, the displacement in z-direction can be determined from the correlation of the sprinkle pattern captured by the cameras (LaVision 2020).

To ensure that the results of this shift are as accurate as possible, both cameras must capture the corresponding images as synchronously as possible. For this purpose, they are connected to a computer with the appropriate software. With the help of this software, signals are sent to both cameras at the same time so that they take the desired images. In the course of this experiment the software "Vic- 3D" is used. The focal length of both cameras is 12mm.

As already mentioned, this image capture should be done on the side faces of the beams. However, the Instron 5582's load frame does not allow the entire side surface of a beam to be captured in orthogonal orientation. This is especially true for the center of the side surface. However, since the greatest deflection is to be expected at the center, this area must be captured by the cameras. Therefore, it is necessary to adjust the setup described in 2.5.1 and 2.5.2 in a way so that about two thirds of the beam can be captured by the cameras. To achieve this, the steel bar is rotated around the z-axis. Since it can be moved freely around this axis, it is fixed in the desired position for this experiment with bolts. This ensures that the angle of the cameras is the same for all experiments
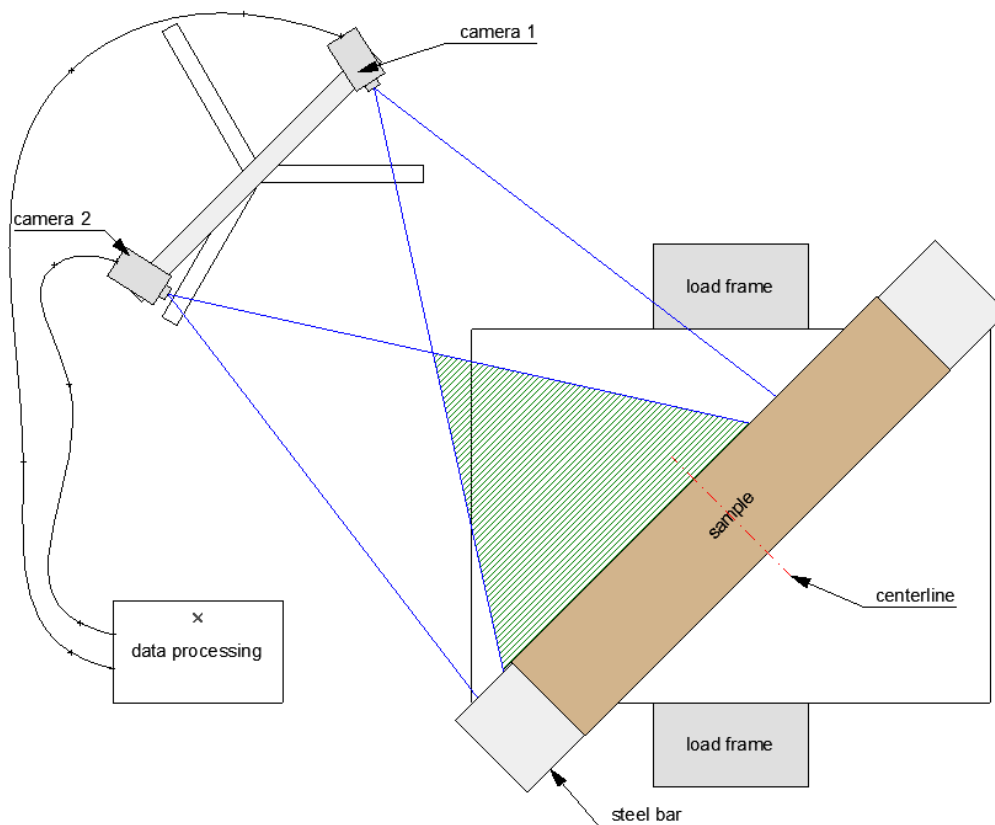
Figure 13: setup 3D digital image correlation
Source: (separate figure, 2020)

To ensure that a homogeneous illumination is cast on the side of the samples, a studio light is positioned behind the camera setup. This illuminates the adjacent brickwork to make the light incidence even more diffuse. In addition, the ceiling lighting is partially switched off to prevent unwanted stray light from disturbing the experiment.

2.6 Instrumentation

The mentioned setup provides a large amount of different and partly independent data. In order to ensure that data is recorded as synchronously as possible and thus prepared for further processing, the corresponding data acquisition must be coordinated.

2.6.1 Displacement in X – Instron 5582

In the course of the individual tests, the Universal Testing System records the flexure load and the associated flexure extension (displacement). With reference to the constant span and the previously entered specimen dimensions in width and depth, the associated software determines the "automatic Young's modulus". Based on this data, a stress-strain diagram is generated. As already mentioned, these results also include compressions in the areas of the supports and the stamp. The data is put out on a ready prepared data sheet as well as raw

data. For this experiment the data sheet includes specimen label, thickness/depth (mm), width (mm), modulus (automatic Young's - Mpa), maximum flexure load (N) and flexure extension at maximum flexure load (mm). The average value is output for the latter.

2.6.2 Displacement in neutral axis – LVDT

For data output the LVDT is connected to a LUCAS ATA 2001 processor amplifier. This in turn passes the data signals to a shielded National Instruments BNC-2110 connector block. This is information exclusively about the position, i.e. the flexure extension. In order to be able to link the flexure load (force) data with the displacement data, force and displacement signals from the Instron 5582 are also transmitted to the connector block. Finally, this connection block is connected to a computer that collects this data and signals and processes them using a program written specifically for this purpose. In the final step, the summarized raw data is output. These include data acquisition time, force, displacement "Instron", and displacement LVDT.

2.6.3 DIC calibration and data acquisition

For the calibration of the setup, standardized charts are used with regularly distributed dots, which are printed black. For this experiment the 28mm plate of *"correlated solutions"* is used. This sheet is placed in the target area of the later test samples and scanned with the two cameras. This process is repeated several times, with the plate being set up in different positions and with different angles and rotations. The data from these images are transferred to the software *"Vic- 3D"*. The system is calibrated based on these images. For this purpose, a separate file is ejected, which serves as a calibration for the later tests.

As already mentioned, DIC records the change of position of single points. However, since these points must have a distinctive character, a sprinkles pattern must be applied to the samples. Make sure that the sprinkle pattern has a high contrast. For this purpose, a sprinkle pattern is applied to the side surfaces of all samples with spray paint, alternating black and white color. When applying the sprinkle pattern, make sure that the paint is not applied over the entire surface, but rather to separate sprinkles. In order to achieve such a surface, individual spray bursts are released from a sufficiently large distance to produce a spray mist that is deposited on the side surfaces of the samples. Ultimately, the surface should resemble television flicker, but with a translucent wooden surface.

In order to check that the sprinkle pattern is sufficiently well recognized and differentiated by the cameras, several shots are taken from one sample, whereby the sample is not stressed during the shots. With the help of the software mentioned above, these photos are evaluated.

The goal here is to maintain the differences of the individual images as low as possible. For this purpose mean and standard deviation of the displacement fields (u,v,w) as well as the transverse and axial strain are evaluated. In the course of this experiment, the worst comparisons of 1-2% of the standard deviation at the position "w" are obtained. The other positions show a deviation of a few per mille. Therefore, it can be assumed that the sprinkle pattern is sufficiently well recognized by the cameras and has a corresponding high contrast.

Figure 14: Example for sprinkle pattern
Source: (separate figure, 2020)

2.7 Test procedure

The bending tests are basically divided into two series. In the first one, the samples are tested according to the 2018 test series, where the mentioned LVDT is also installed. In the second part the samples are subjected to a bending test until failure and a subsequent investigation of the cause.

Before the tests, the center axis of all samples is marked normal to the longitudinal axis. For this purpose, the opposite corner points of a side surface are connected. A line is drawn from this intersection/center point normal to the longitudinal axis to the top and bottom of the samples. This line is copied outwards along the longitudinal axis in both directions parallel by 25 mm. In total this corresponds to the width of the steel plate. These lines are then transferred to the top side of the samples and extended to the opposite edge perpendicular to the longitudinal axis. These two lines now mark the later position of the steel plate and the lowered stamp. The pinboard needle for the LVDT will also be attached to the center of the side surface. In addition, two points along the longitudinal axis must be set from this center point, which mark the position of the bearing rollers and the screws on which the LVDT yoke is placed. Also, from these two points a normal line has to be drawn along the longitudinal axis.

2.7.1 Non-destructive

To verify the results of the 2018 test and to determine if storage for more than 15 months would have an effect on this, 4 samples were tested with all possible core lamella widths. For this purpose the following samples are examined:

- B4E09-12 (35mm core lamellas)
- C1B01-04 (140mm core lamellas)
- C2C05-08 (70mm core lamellas)
- C4F05-08 (35mm core lamellas)

For this test series, the samples are subjected to a 3-point flexure test using the Instron 5582 Universal Testing System. The span width is 711.2 mm (28 in). The samples are centered on the bearing rollers. The steel plate on the top of the samples is then placed on the center axis. The stamp is lowered onto this steel plate and loaded with 100-200 N to secure the position. The maximum force during this test series is approx. 4150 N. The rate of loading is set at 1mm per minute. Each test run has to be assigned the corresponding sample coding and the exact dimensions. In addition, the file name must indicate that it is a non-destructive test.

For the determination of the deformation along the zero line, without influence of compressions, the LVDT is also switched on. For this purpose the aluminum yoke is mounted on the sample as described in 2.5.2 For each sample, check that the core extension can be moved without resistance. Since it cannot be guaranteed that the core extension has the same zero position for all samples, the offset of the LVDT must be adjusted. First set the offset to zero and then use the negative value of the zero position as the new offset. In addition, it is important that the data logger is opened before each test and closed at the end of the test.

After these 4 samples have been examined and compared with the results of the previous tests, all other samples are subjected to the same test procedure. In this case the DIC is additionally included in the test. Before starting the test make sure that photos (4-6) of the samples are taken in the unloaded state. These serve as a later verification of the sprinkle pattern. The stamp is then lowered onto the sample and loaded until it is secured in position (~100- 200 N). Also, in this state the sample has to be taken. The same applies to the time after reaching the maximum load of about 4150 N. During the non-destructive test a photo is taken every 10 seconds.

2.7.2 Destructive

After completion of the non-destructive test, each sample shall be tested to failure. For this purpose, each sample is subjected to a destructive test immediately after completion of the final non-destructive test. Therefore, the span is 711.2 mm (28 in) and the loading rate is again 1mm/min. Similar to the non-destructive test, the steel plate is placed on the sample and loaded with 100-200 N. However, no LVDT is used in this test series, so the yoke must be removed from the sample and stowed away in such a way that it cannot be damaged in the course of the destructive test. Again, each individual file must be marked with the encoding of the corresponding sample, but to mark it in a way that it can be recognized as a destructive test.

The DIC is also used in this test series. Compared to the previous test, a photo is to be taken in the positionally secured state and in the final stage (failed sample). During the test, photographs are to be taken every 30 seconds up to a load of approximately 15,000 to 18,000 N and then every 15 seconds until failure. Increasing the frame rate at the end of the test is used to better track deformations and compressions.

At the end of the test, the sample is examined, and the nature of the failure is determined. Here we distinguish between three types.

- failure of glue line
- failure of wood
- combination of both

In order to be able to trace these points of failure even in unloaded condition, they are marked with lines.

2.8 Analysis

As described above, the test results have to be compared with the standard values of the PRG 320 in order to estimate whether CLT panels with smaller core lamellas than those specified by the PRG 320 will reach these limits. This requires further calculations in addition to the analysis of the bending tests. Since the calculations are performed with SI units, the standard values of the PRG 320 refer to the tables A3 and A4.

2.8.1 Modulus of Inertia - MOI

The modulus described in point 2.6.1 refers to a homogeneous material cross-section. However, this is not given with CLT panels due to the different orientation of the individual lamellas. Looking at the elastic ratio between radial to longitudinal and tangential to

longitudinal direction of Ponderosa Pine, the ratio is between 0.083 and 0.122 (Ross; USDA Forest Service. 2010).

Due to this heterogeneous structure of the samples, the modulus of inertia (MOI) differs from that of a beam with a homogeneous cross-section. To determine the influence of this, the results of the actual, heterogeneous carriers are compared with those of the theoretical, homogeneous ones. It should be noted that the fundamental inhomogeneity of wood as a material is neglected. For homogeneous beams the following formula is used

Formula 2: calculation of MOI for a homogenous beam

$$I = \frac{b * d^3}{12} \ [mm^4]$$

I *Modulus of Inertia in mm⁴*

b *width in mm*

d *depth in mm*

In the case of a heterogeneous sample, this is converted into an ideal cross-section with uniform material properties. For this purpose, the areas of the individual lamellas cross sections are determined first, whereby those of the core lamellas are multiplied by the above mentioned ratio. For this experiment the ratio of 0.083 is used. Since the cross-section is 2 axis symmetrical, the center of gravity is in the center of the cross-section. In the next step, the distances of the centers of gravity of the individual layers to the edge of the beam are determined. Using these values, the MOI of a heterogeneous beam can be determined using the following formula.

Formula 3: calculation of MOI for a heterogenous beam

$$I^* = I_y^{(1)} + A^{(1)} * (z_s^{(1)} - z_s^*)^2 + n^{(2)} * I_y^{(2)} + A^{(2)} * n^{(2)} * \left(z_s^{(2)} - z_s^*\right)^2 + I_y^{(2)} + A^{(2)} * (z_s^{(2)} - z_s^*)^2$$

I^* *– Modulus of Inertia for a heterogenous beam in mm⁴*

$I^{(n)}{}_y$ *– Modulus of Inertia for different lamellas in mm⁴*

$A^{(n)}$ *– Area of different lamellas in mm²*

$z^{(n)}{}_s$ *– center of gravity of different lamellas*

$z^*{}_s$ *– center of gravity of the whole beam*

$n^{(n)}$ *– ratio between different MOE*

The same procedure is applied to the gaps between the lamellas of the top layers.

2.8.2 Modulus of Elasticity - MOE

It is essential to compare the results of the tests with the standard values of the PRG 320. However, since PRG 320 only lists the bending stiffness of the individual grades, the data and formulas provided must be used to calculate back to the respective Modulus of Elasticity. Since the samples of the test series do not correspond to the dimensions of the standard beams, it must first be checked whether the bending stiffness of a beam with the dimensions of the samples correspond to those of the PRG 320. The formula provided by PRG 320 is used for this (PRG 320:2019).

Formula 4: calculation of flatwise bending stiffness of CLT panels

$$(EI)_{eff,0} = \sum_{i=1}^{n} E_i b_0 \frac{t_i^3}{12} + \sum_{i=1}^{n} E_i b_0 t_i z_i^2$$

$(EI)_{eff,0}$ *Effective flatwise bending stiffness of CLT in Nmm²*

E_i *Modulus of Elasticity of the lamination in the i-th layer in MPa*

b_0 *CLT width in the CLT major strength direction in mm*

t_i *thickness of laminations in the i-th layer, in mm*

z_i *distance between the center point of the i-th layer and the neutral axis in mm*

n *number of layer in the CLT*

Then the generally valid formula for the bending stiffness has to be transformed in such a way that the section modulus is deducted and the modulus of elasticity is separated. Formula 2 is used for the modulus of elasticity.

The formula of ASTM D198-15 is used to calculate the modulus of elasticity of the tested samples (ASTM D198:2015).

Formula 5: calculation of apparent Modulus of Elasticity

$$E_{app} = \frac{Pl^3}{4bd^3\Delta}$$

E_{app} *Apparent Modulus of Elasticity in N/mm²*

P *Increment of applied load below proportional limit in N*

l *Span in mm*

b *width of specimen in mm*

d *depth of specimen in mm*

Δ *Increment of deflection of neutral axis in mm*

Since this formula again refers to a homogeneous component, the modulus of elasticity is additionally calculated with the section modulus of a heterogeneous beam as a comparison

value. For this purpose, the generally valid formula for calculating the maximum deflection of a beam on two supports with a central load is transformed.

Formula 6: calculation of deflection

$$w = \frac{Pl^3}{48EI} \rightarrow E = \frac{Pl^3}{48wI}$$

E   *Modulus of Elasticity in N/mm²*

P   *Increment of applied load below proportional limit in N*

l   *Span in mm*

I   *Modulus of Inertia in mm⁴*

w   *Increment of deflection of neutral axis in mm*

2.8.3 Modulus of Rupture - MOR

For the second part of the test series, the bend test until failure of the samples, it is also necessary to determine the results of comparison samples based on the standard value of PRG 320. As a first step, the flatwise bending moment must be determined. For this purpose the corresponding formula of PRG 320 is used (PRG 320:2019).

Formula 7: calculation of flatwise bending moment of CLT panels

$$(f_b S)_{eff,0} = 0{,}85 f_{b,major} S_{eff,0}$$

$(f_bS)_{eff,0}$ *Effective LSD flatwise bending moment resistance of CLT in Nmm*

$f_{b,major}$ *LSD specified bending strength of the lamination in the CLT major strength direction in MPa*

$S_{eff,o}$ $\frac{(EI)_{eff,0}}{E_{major}}\frac{2}{t_p}$ *in mm³ in the CLT major strength direction*

$(EI)_{eff,0}$ *Effective flatwise bending stiffness of CLT in Nmm²*

E_{major} *ASD or LSD modulus of elasticity of th lamination in MPs*

t_p *gross thickness of CLT in mm*

Then, the generally valid formula for determining the bending stiffness is transformed to finally obtain the modulus of rupture for the comparison samples.

Formula 8: calculation of flexural strength

$$\sigma = \frac{(f_b S)_{eff,0}}{W} \rightarrow \sigma = \frac{(f_b S)_{eff,0} * 6}{bd^2}$$

σ *flexural strength (Modulus of Rupture) in N/mm²*

$(f_bS)_{eff,0}$ *Effective LSD flatwise bending moment resistance of CLT in Nmm*

W   *Section Modulus mm³*

b   *width of specimen in mm*

d   *depth of specimen in mm*

The formula of ASTM D198-15 is used to calculate the modulus of rupture of the tested samples (ASTM D198:2015).

Formula 9: calculation of Modulus of Rupture

$$S_R = \frac{3P_{max}l}{2bd^2}$$

SR   *Modulus of Rupture in N/mm²*

Pmax   *Maximum load borne by specimen loaded to failure in N*

l   *Span in mm*

b   *width of specimen in mm*

d   *depth of specimen in mm*

2.8.4 Slope – "k"

Subsequently, the slope of the test results of the individual samples is determined for both the modulus of elasticity and the modulus of rupture. For the modulus of elasticity, the range from 2000 to 4000 N is considered here. For the modulus of rupture, the consideration is limited to the results from 1000 N until the failure of the samples. For the determination of the corresponding slope, the respective values are now compared to those of the corresponding deflection. First the lower limit value is subtracted from the upper limit value of the load, then the same procedure with the values of the deflection. Finally, the two difference values are divided, whereby the deflection represents the dividend. This results in the unit *"N/mm"* for the slope.

3   Results and Discussion

The results of the two bending tests and their evaluation are explained in the following points.

3.1   Comparison sample

Since the examined samples and thus also the theoretical comparison sample deviate from the dimensions of the standard values of the PRG 320, such a calculation is made using the above formulas. On the basis of the basic values and the dimensions of the samples specified in the PRG 320, the following values result for the individual classifications. The average dimensions of the samples have a width of 154mm and a support length of 711.2mm. The sample depth consists of three layers of 23.67mm each, resulting in a total depth of 71mm. When determining the values and comparing them with those of the PRG 320, it was found that with flatwise bending stiffness, the load-bearing effect of the lamellas arranged normal to the main load-bearing direction (core lamellas) is not taken into account in the calculation.

Table 2: Values for comparison samples based on PRG 320 standards
source: (own table, 2020)

CLT Grade	$(EI)_{eff,0}$ Nmm²	E N/mm²	$(f_bS)_{eff,0}$ Nmm	σ_{max} N/mm²
E1	$51{,}75 \times 10^6$	11267	$2{,}99 \times 10^6$	23,08
E2	$45{,}56 \times 10^6$	9919	$2{,}53 \times 10^6$	19,65
E3	$36{,}71 \times 10^6$	7993	$1{,}84 \times 10^6$	14,24
E5	$45{,}56 \times 10^6$	9919	$2{,}53 \times 10^6$	19,46
V1(N)	$48{,}65 \times 10^6$	10593	$1{,}06 \times 10^6$	8,19
V2	$42{,}02 \times 10^6$	9148	$1{,}25 \times 10^6$	9,66
V5	$48{,}65 \times 10^6$	10593	$1{,}16 \times 10^6$	9,00

Since the first 4 classifications apply to machine stress rated lumber, they are not used as comparative values. For the remaining 3 classes "V1(N)" refers to douglas fir and larch lumber, "V2" to spruce-pine-fir lumber and "V3" to hem-fir. Since the grade "V2" represents a relatively large group and thus the standard values cover a large range, these determined values are used as comparison values.

3.2   Comparison homogeneous and heterogeneous results

As described in point 2.8 and the corresponding sub points, the calculations are determined for a homogeneous as well as for a heterogeneous cross-section of the samples.

The comparison of the values of the modulus of inertia shows that samples with a theoretically homogeneous cross section give better values by 3.56 to 3.71% than those with the heterogeneous one.

For the comparison of the values of the modulus of elasticity there are deviations from homogeneous to heterogeneous cross section of -5.31 to 6.79%. However, the average is -3.75% and the upper deviation of 6.79% is a one-time deviation of such magnitude.

The consideration of the values for the modulus of rupture behaves similar to the modulus of inertia, whereby these values show a negative sign. Thus, the deviation of the heterogeneous and homogeneous results lies between -3.69 and -3.98%.

On the basis of these results, it can be seen that the differences in the results between heterogeneous and homogeneous cross sections are at worst ±5% or less. Therefore, the values based on the formulas of ASTM D198-15 are used for further calculations and analysis of their results.

3.3   Results of bending tests

After completion of the two series of bending tests, the results are compared using statistical methods. Since the samples with 140mm wide core lamellas meet the requirement for the ratio of lamella width to height, they serve as a reference for the comparison with the other two core lamella widths.

3.3.1   T-test

To verify whether the comparisons of the individual results of the samples with respect to the width of the core lamellas can be considered equivalent from a statistical point of view, the 5% percentile is used as a limit value. This means that the results of the t-tests should be between 1.0 and 0.05.

For the non-destructive tests the following values of the t-tests are obtained.

- 140 to 70 mm → 0,187
- 140 to 35 mm → 0,654

From this it can be concluded that the results of the non-destructive tests can be considered statistically equivalent.
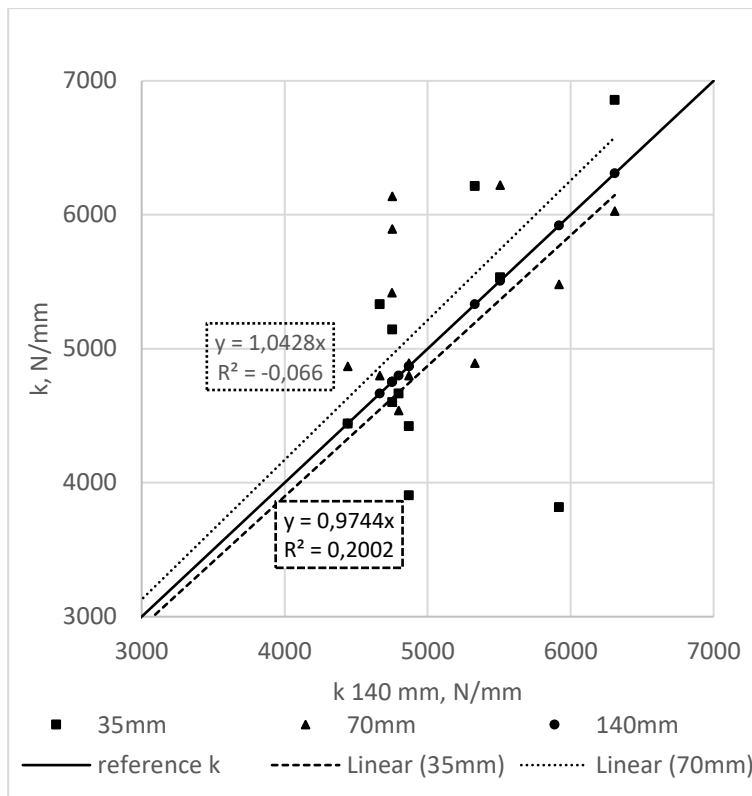
Figure 15: Comparison of core lamella width of non-destructive bending results
Source: (separate figure, 2020)

The values of the destructive tests provide the following t-test results.

- 140 to 70 mm → 0,531
- 140 to 35 mm → 0,021

This shows that the values of the 70mm samples can be regarded as equivalent. However, the result of the 35mm test is below the threshold of 5% and is therefore not equivalent. Nevertheless, these results will be used for further investigations.
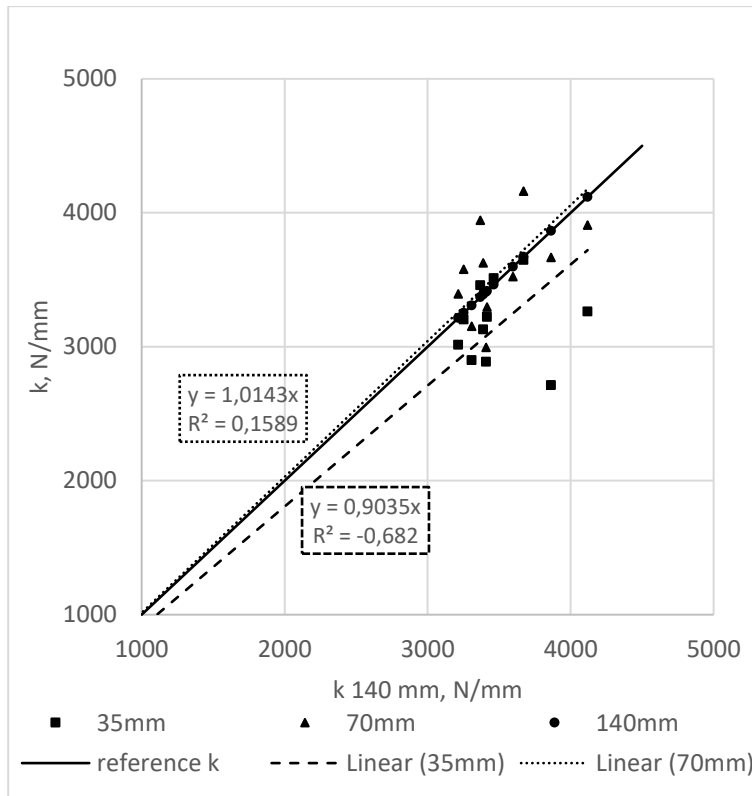
Figure 16: Comparison of core lamella width of destructive bending results
Source: (separate figure, 2020)

3.3.2 Comparison with PRG 320

The next step is to compare the tested results with the standard values of the PRG 320. A distinction is made between the different widths of the core lamellas and the original panels.

The values of the modulus of elasticity clearly show that the samples of panel B only occasionally reach the required values of PRG 320. This also applies to the samples of panel C with a core lamella width of 140mm. Only the samples with a core lamella width of 35 and 70mm of panel C exceed the limit for the most part. Furthermore, the samples with 35 and 70mm, in contrast to those with 140mm, show a high scatter.
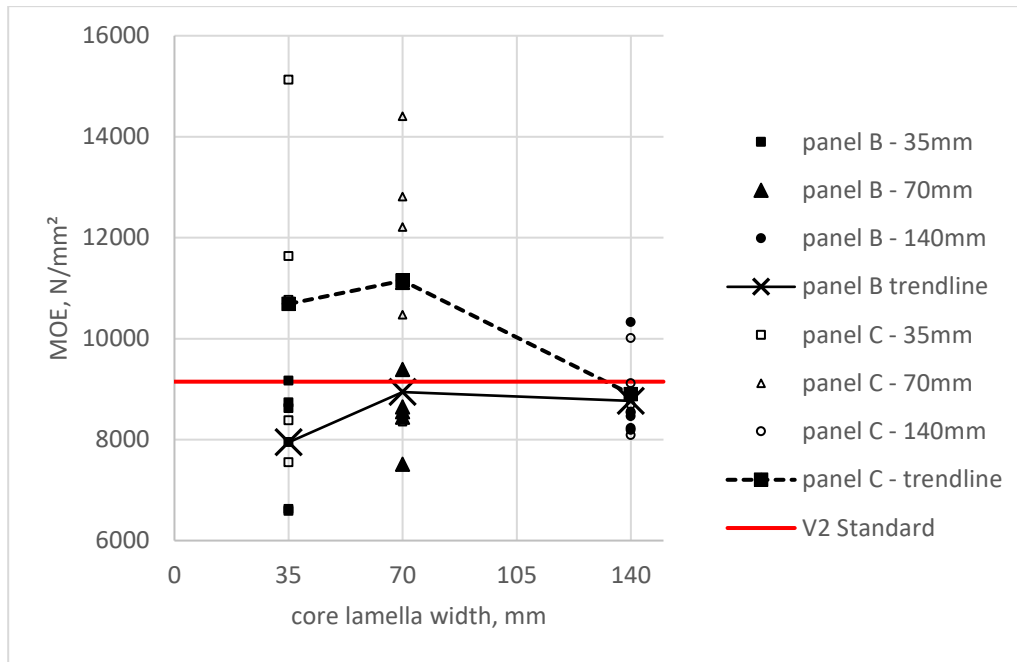
Figure 17: MOE panel comparison with PRG 320
Source: (separate figure, 2020)

When comparing the values of the modulus of rupture with the standard value of the PRG 320 for , it should be noted that a safety factor of 2.1 must be added to this (ASTM D1990:2019).
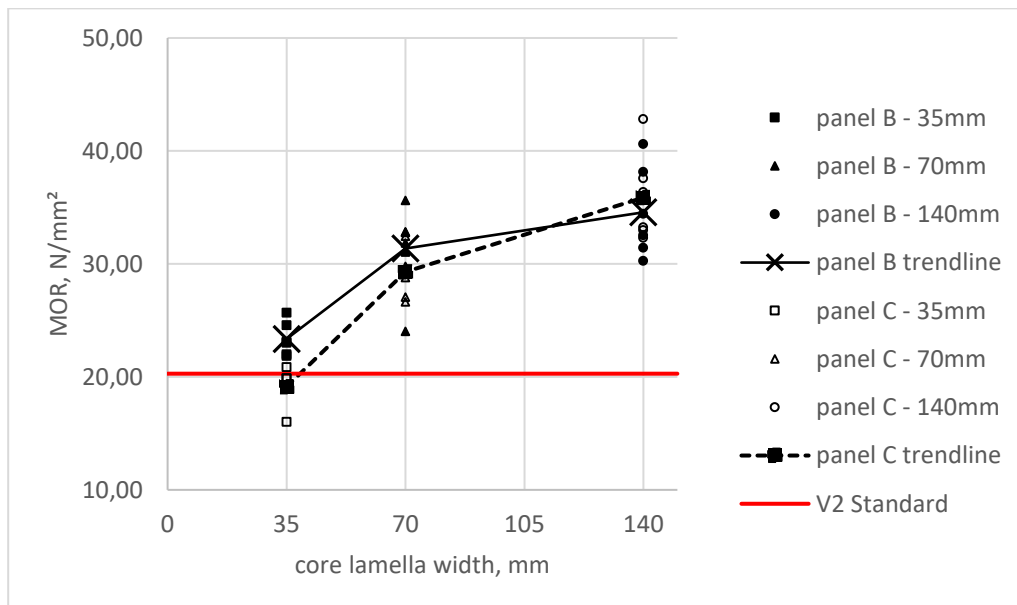
Figure 18:MOR panel comparison with PRG 320
Source: (separate figure, 2020)

3.3.3 Type of failure

In order to find a relation between the values of the modulus of rupture and the type of failure, the results are assigned to the described types of failure. Afterwards, these are normally distributed to determine whether there is a cluster formation. Those values with the addition "gf" describe samples where the failure occurs along the glueline. In the remaining samples the wood or the combination of both failed.
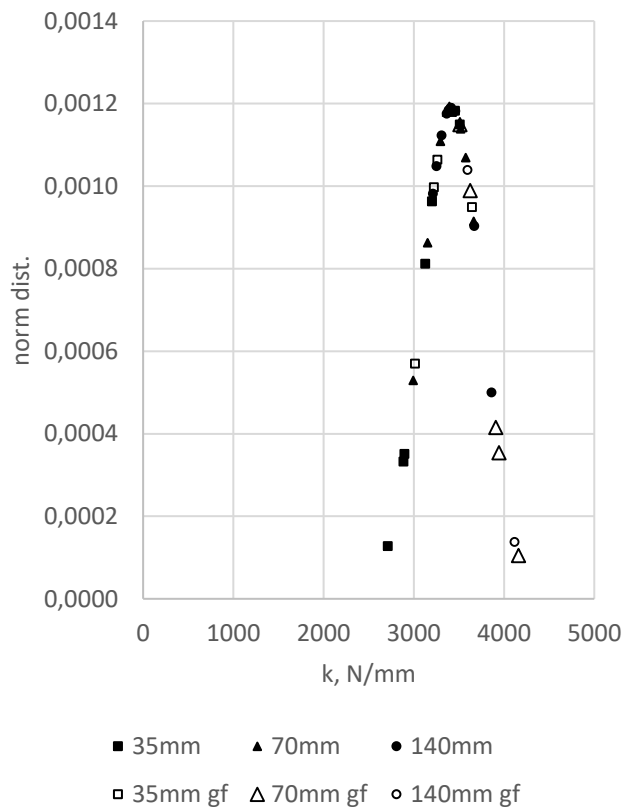
Figure 19: normal distribution of failure type
Source: (separate figure, 2020)

Looking at the curve, a cluster appears in the area of the central axis with individual values above and below it. Looking at the type of failure, it can be seen that those samples with glueline failure are located at the upper half of the curve. This shows that these samples reach very high modulus of rupture values, but with such a large number of samples with glueline failure this may be a sign that the resin has not set properly. Otherwise the glueline should be more resistant than wood itself.

3.4 DIC strain maps

Examination of the data from the DIC images shows that the sprinkle pattern is easily recognizable and can also be captured by the corresponding software. The strain maps show the influence of the load on the samples and where which deformations occur. However, an exact analysis of these images is still pending and has to be done in further projects.
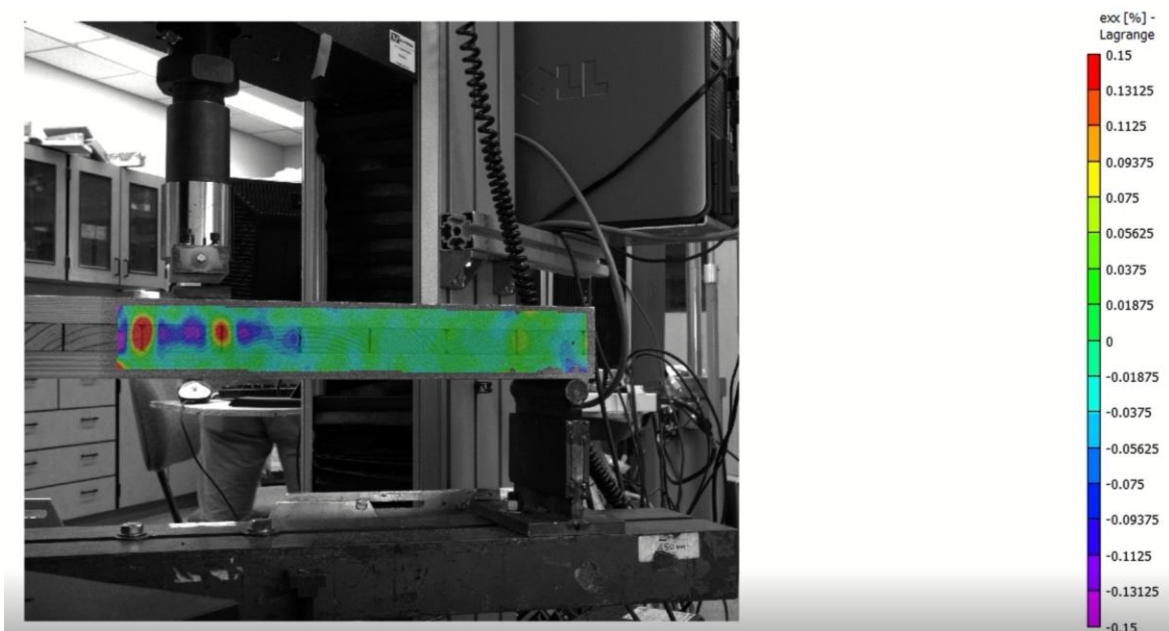
Figure 20: strain map exx of sample C2D05-08
Source: (separate figure, 2020)

4   Conclusion

The above mentioned calculations and their evaluations show that the results regarding Modulus of Elasticity and Modulus of Rupture are in part very contrary. Especially for Modulus of Elasticity it is clearly visible that there is a significant difference between the individual panels, especially in the narrower core lamellas. This significant difference between the individual panels and the low values of the samples with 140mm wide core lamellas indicates that the test series should be repeated to verify these results.

This is in contrast to the results of the Modulus of Rupture. With a few exceptions, all samples exceeded the required minimum value of PRG 320. However, the samples with the narrower core lamellas show that there is a difference between the original panels. If the type of failure is also taken into account, it becomes apparent that the production of the panels did not run smoothly and therefore the desired quality could not be achieved.

In a broader sense, the DIC images still need to be analyzed. This concerns especially the behavior of the individual samples during the tests.

On the basis of these results, it is clear that a reduction of the core lamella width to a further reduction is to be pursued. Especially those samples with 70mm wide core lamellas show good values compared to the standard values of the PRG 320. A further reduction towards 35mm can also provide attractive results. However, it has to be said in general that for an introduction to the wood market economy, and therefore also to PRG 320, reproductions of this test series are required. Other width to depth ratios should also be considered in order to achieve maximum performance with the narrowest possible core lamellas.

5 Directories

5.1 List of references

5.1.1 Bibliography

American National Standard (2019): PRG 320, Standard for Performance-Rated Cross-Laminated Timber.

ASTM International (2015): ASTM D198, Standard Test Methods of Static Tests of Lumber in Structural Sizes.

ASTM International (2019): ASTM D1990, Standard Practice for Establishing Allowable Properties for Visually-Graded Dimension Lumber from In-Grade Tests of Full-Size Specimens.

LaVision (2020): 2D-/3D Stereo Digital Image Correlation, online verfügbar: www.lavision.de/en/applications/materials-testing/stereo-dic/index.php, (Stand: 22.08.2020).

Prox Lauren, et al. (2018): unpublished data.

Ross, R. J. & F. P. L. USDA Forest Service. (2010): Wood handbook : wood as an engineering material. Madison, WI.

5.2 List of figures

5.3   List of tables

5.4   List of directory

35

5.5 List of abbreviation

CLT – Cross laminated timber

SOP – Standard Operating Procedure

SDS – Safety Data Sheet

MOE – Modulus of Elasticity

MOR – Modulus of Rupture

6   Annex

Annex 1 - SOP for CLT Production at Oregon State University

Annex 2 – SDS for Cascophen LT-75C

Annex 3 – SDS for Cascoset FM-282